

3. F. H. Shu, H. Shang, A. E. Glassgold, T. Lee, *Science* **277**, 1475 (1997).
4. B. S. Meyer, in *Chondrites and the Protoplanetary Disk*, A. N. Krot, E. R. D. Scott, B. Reipurth, Eds. (Astrophysical Society of the Pacific, San Francisco, CA, 2005), pp. 515–526.
5. S. Tachibana, G. R. Huss, N. T. Kita, G. Shimoda, Y. Morishita, *Astrophys. J.* **639**, L87 (2006).
6. S. Mostefaoui, G. W. Lugmair, P. Hoppe, *Astrophys. J.* **625**, 271 (2005).
7. A. Shukolyukov, G. W. Lugmair, *Earth Planet. Sci. Lett.* **119**, 159 (1993).
8. M. Bizzarro, J. A. Baker, H. Haack, K. L. Lundgaard, *Astrophys. J.* **632**, L41 (2005).
9. A. N. Halliday, T. Kleine, in *Meteorites and the Early Solar System II*, D. S. Lauretta, H. Y. McSween, Eds. (Univ. of Arizona Press, Tucson, AZ, 2006), pp. 775–801.
10. N. Kita *et al.*, in *Chondrites and the Protoplanetary Disk*, A. N. Krot, E. R. D. Scott, B. Reipurth, Eds. (Astrophysical Society of the Pacific, San Francisco, CA, 2005), pp. 558–587.
11. Materials and methods are available as supporting material on Science Online.
12. Y. Amelin, A. N. Krot, I. D. Hutcheon, A. A. Ulyanov, *Science* **297**, 1678 (2002).
13. J. Baker, M. Bizzarro, N. Wittig, J. Connelly, H. Haack, *Nature* **436**, 1127 (2005).
14. Y. Amelin, *Lunar Planet. Sci.* **XXXVIII**, 1669 (abstr.) (2007).
15. J. A. Baker, M. Bizzarro, abstract 8612 presented at the *Protostars and Planets V* meeting, Hilton Waikoloa Village, HI, 24 to 28 October 2005.
16. A. Trinquier, J.-L. Birck, C. Allègre, *Astrophys. J.* **655**, 1179 (2007).
17. J. H. Jones, M. J. Drake, *Geochim. Cosmochim. Acta* **47**, 1199 (1983).
18. K. Thrane, M. Bizzarro, J. A. Baker, *Astrophys. J.* **646**, L159 (2006).
19. A. Palacios *et al.*, *Astron. Astrophys.* **429**, 613 (2005).
20. M. Limongi, A. Chieffi, *Astrophys. J.* **647**, 483 (2006).
21. M. Arnoult, S. Gorieli, G. Meynet, *Astron. Astrophys.* **453**, 653 (2006).
22. G. Meynet, A. Maeder, *Astron. Astrophys.* **429**, 581 (2005).
23. D. P. Glavin, A. Kubny, E. Jagoutz, G. W. Lugmair, *Meteorit. Planet. Sci.* **39**, 693 (2004).
24. A. Markowski *et al.*, *Meteorit. Planet. Sci.* **41**, 5195 (abstr.) (2006).
25. J. J. Hester, S. J. Desch, in *Chondrites and the Protoplanetary Disk*, A. N. Krot, E. R. D. Scott, B. Reipurth, Eds. (Astrophysical Society of the Pacific, San Francisco, CA, 2005), pp. 107–130.
26. J. M. Rathborne *et al.*, *Mon. Not. R. Astron. Soc.* **331**, 85 (2002).
27. N. Ouellette, S. J. Desch, J. J. Hester, L. A. Leshin, in *Chondrites and the Protoplanetary Disk*, A. N. Krot, E. R. D. Scott, B. Reipurth, Eds. (Astrophysical Society of the Pacific, San Francisco, CA, 2005), pp. 527–538.
28. A. P. Boss, *Meteorit. Planet. Sci.* **41**, 1695 (2006).
29. S. E. Woosley, *Astrophys. J.* **476**, 801 (1997).
30. M. J. Drake, K. Righter, *Nature* **416**, 39 (2002).
31. A. Shukolyukov, G. W. Lugmair, *Lunar Planet. Sci.* **XXXVII**, 1478 (abstr.) (2006).
32. Financial support for this project was provided by the Danish National Science Foundation, NASA's Cosmochemistry Program, and the Danish Natural Science Research Council.

#### Supporting Online Material

www.sciencemag.org/cgi/content/full/316/5828/1178/DC1  
Materials and Methods

SOM Text

Tables S1 and S2

References

8 February 2007; accepted 27 March 2007

10.1126/science.1141040

# Model Projections of an Imminent Transition to a More Arid Climate in Southwestern North America

Richard Seager,<sup>1\*</sup> Mingfang Ting,<sup>1</sup> Isaac Held,<sup>2,3</sup> Yochanan Kushnir,<sup>1</sup> Jian Lu,<sup>4</sup> Gabriel Vecchi,<sup>2</sup> Hwei-Ping Huang,<sup>1</sup> Nili Harnik,<sup>5</sup> Ants Leetmaa,<sup>2</sup> Ngar-Cheung Lau,<sup>2,3</sup> Cuihua Li,<sup>1</sup> Jennifer Velez,<sup>1</sup> Naomi Naik<sup>1</sup>

How anthropogenic climate change will affect hydroclimate in the arid regions of southwestern North America has implications for the allocation of water resources and the course of regional development. Here we show that there is a broad consensus among climate models that this region will dry in the 21st century and that the transition to a more arid climate should already be under way. If these models are correct, the levels of aridity of the recent multiyear drought or the Dust Bowl and the 1950s droughts will become the new climatology of the American Southwest within a time frame of years to decades.

The Third Assessment Report of the Intergovernmental Panel on Climate Change (IPCC) reported that the average of all the participating models showed a general decrease in rainfall in the subtropics during the 21st century, although there was also considerable disagreement among the models (1). Subtropical drying accompanying rising CO<sub>2</sub> was also found in the models participating in the second Coupled Model Intercomparison Project (2). We examined future subtropical drying by analyzing the time history of precipitation in 19 climate models participating in the Fourth Assessment Report

(AR4) of the IPCC (3). The future climate projections followed the A1B emissions scenario (4), in which CO<sub>2</sub> emissions increase until about 2050 and decrease modestly thereafter, leading to a CO<sub>2</sub> concentration of 720 parts per million in 2100. We also analyzed the simulations by these models for the 1860–2000 period, in which the models were forced by the known history of trace gases and estimated changes in solar irradiance, volcanic and anthropogenic aerosols, and land use (with some variation among the models). These simulations provided initial conditions for the 21st-century climate projections. For each model, climatologies were computed for the 1950–2000 period by averaging over all the simulations available for each model. All climate changes shown here are departures from this climatology.

We define an area (shown as a box in Fig. 4A) called “the Southwest” (including all land between 125°W and 95°W and 25°N and 40°N) that incorporates the southwestern United States and parts of northern Mexico. Figure 1 shows the modeled history and future of the annual mean

precipitation minus the evaporation ( $P - E$ ), averaged over this region for the period common to all of the models (1900–2098). The median, 25th, and 75th percentiles of the model  $P - E$  distribution and the median of  $P$  and  $E$  are shown. For cases in which there were multiple simulations with a single model, data from these simulations were averaged together before computing the distribution.  $P - E$  equals the moisture convergence by the atmospheric flow and (over land) the amount of water that goes into runoff.

In the multimodel ensemble mean, there is a transition to a sustained drier climate that begins in the late 20th and early 21st centuries. In the ensemble mean, both  $P$  and  $E$  decrease, but the former decreases by a larger amount.  $P - E$  is primarily reduced in winter, when  $P$  decreases and  $E$  is unchanged or modestly increased, whereas in summer, both  $P$  and  $E$  decrease. The annual mean reduction in  $P$  for this region, calculated from rain gauge data within the Global Historical Climatology Network, was 0.09 mm/day between 1932 and 1939 (the Dust Bowl drought) and 0.13 mm/day between 1948 and 1957 (the 1950s Southwest drought). The ensemble median reduction in  $P$  that drives the reduction in  $P - E$  reaches 0.1 mm/day in midcentury, and one quarter of the models reach this amount in the early part of the current century.

The annual mean  $P - E$  difference between 20-year periods in the 21st century and the 1950–2000 climatology for the 19 models are shown in Fig. 2. Almost all models have a drying trend in the American Southwest, and they consistently become drier throughout the century. Only 1 of the 19 models has a trend toward a wetter climate. Of the total of 49 individual projections conducted with the 19 models, even as early as the 2021–2040 period, only 3 projections show a shift to a wetter climate. Examples of modeled history and future precipitation for single simulations of four individual models are shown in Fig. 3 and provide an idea of potential trajectories toward the more arid climate.

<sup>1</sup>Lamont Doherty Earth Observatory (LDEO), Columbia University, Palisades, NY 10964, USA. <sup>2</sup>National Oceanic and Atmospheric Administration (NOAA) Geophysical Fluid Dynamics Laboratory, Princeton, NJ 08540, USA. <sup>3</sup>Program in Atmospheric and Oceanic Sciences, Department of Geosciences, Princeton University, Princeton, NJ 08544, USA. <sup>4</sup>National Center for Atmospheric Research, Boulder, CO 80307, USA. <sup>5</sup>Tel Aviv University, Tel Aviv, Israel.

\*To whom correspondence should be addressed. E-mail: seager@ldeo.columbia.edu

The contours in Fig. 4, A to C, show a map of the change in  $P - E$  for the decades between 2021 and 2040 minus those in the 1950–2000 period for one of the IPCC models: the Geophysical Fluid Dynamics Laboratory (GFDL) climate model CM2.1 (5). In general, large regions of the relatively dry subtropics dry further, whereas wetter, higher-latitude regions become wetter still. In addition to the American Southwest, the southern Europe–Mediterranean–Middle East region also experiences a severe drying. This pattern of subtropical drying and moistening at higher latitudes is a robust feature of current projections with different models of future climate (6).

The change ( $\delta$ ) in  $P - E$  (in meters per second) is balanced by a change in atmospheric moisture convergence, namely

$$\rho_w g \delta(P - E) = -\delta \left[ \int_0^{p_s} \nabla \cdot (\overline{uq}) dp + \int_0^{p_s} \nabla \cdot (\overline{u'q'}) dp \right] \quad (1)$$

Overbars indicate monthly means, primes represent departures from the monthly mean,  $\rho_w$  is the density of water,  $g$  indicates the acceleration due to gravity, and  $\nabla$  indicates the horizontal divergence operator. The change in moisture con-

vergence can be divided into contributions from the mean flow and from eddies. In the former, the atmospheric flow ( $\overline{u}$ ) and the moisture ( $\overline{q}$ ) are averaged over a month before computing the moisture transport, whereas the latter is primarily associated with the highly variable wind ( $u'$ ) and moisture ( $q'$ ) fields within storm systems. The moisture convergence is integrated over the pressure ( $p$ ) from the top of the atmosphere ( $p = 0$ ) to the surface ( $p_s$ ). The mean wind and humidity fields in Eq. 1 can be taken to be their climatological fields. (The rectification of interannual variability in the monthly mean flow and moisture fields is found to be negligible.) Changes in the mean flow contribution can, in turn, be approximated by one part associated with the climatological circulation from 1950 to 2000 ( $\overline{u}_p$ ), operating on the increase in climatological atmospheric humidity ( $\delta \overline{q}$ , a consequence of atmospheric warming), and by another part due to the change in circulation climatology ( $\delta \overline{u}$ ), operating on the atmospheric humidity climatology from 1950 to 2000 ( $\overline{q}_p$ ). The nonlinear term involving changes in both the mean flow and the moisture field is found to be relatively small. Hence, Eq. 1 can be approximated by:

$$\rho_w g \delta(P - E) \sim - \int_0^{p_s} \nabla \cdot (\overline{q}_p \delta \overline{u} + \overline{u}_p \delta \overline{q}) dp - \delta \int_0^{p_s} \nabla \cdot (\overline{u'q'}) dp \quad (2)$$

We therefore think in terms of a threefold decomposition of  $P - E$ , as displayed in Fig. 4 (colors) for the GFDL CM2.1 model: (i) a contribution from the change in mean circulation, (ii) a contribution from the change in mean humidity, and (iii) a contribution from eddies.

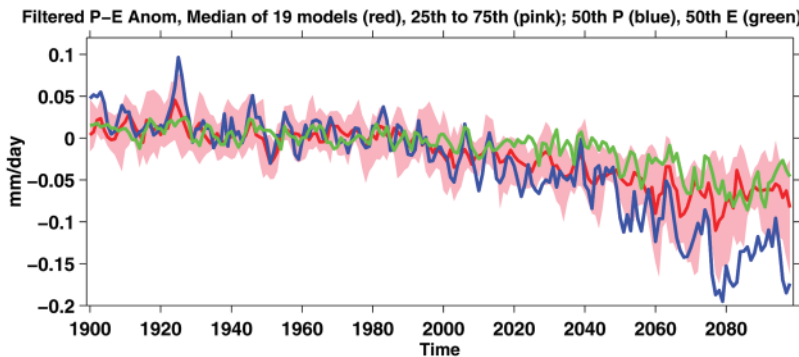


**Fig. 1.** Modeled changes in annual mean precipitation minus evaporation over the American Southwest (125°W to 95°W and 25°N to 40°N, land areas only), averaged over ensemble members for each of the 19 models. The historical period used known and estimated climate forcings, and the projections used the SResA1B emissions scenario. The median (red line) and 25th and 75th percentiles (pink shading) of the  $P - E$  distribution among the 19 models are shown, as are the ensemble medians of  $P$  (blue line) and  $E$  (green line) for the period common to all models (1900–2098). Anomalies (Anom) for each model are relative to that model's climatology from 1950–2000. Results have been 6-year low-pass Butterworth-filtered to emphasize low-frequency variability that is of most consequence for water resources. The model ensemble mean  $P - E$  in this region is around 0.3 mm/day.

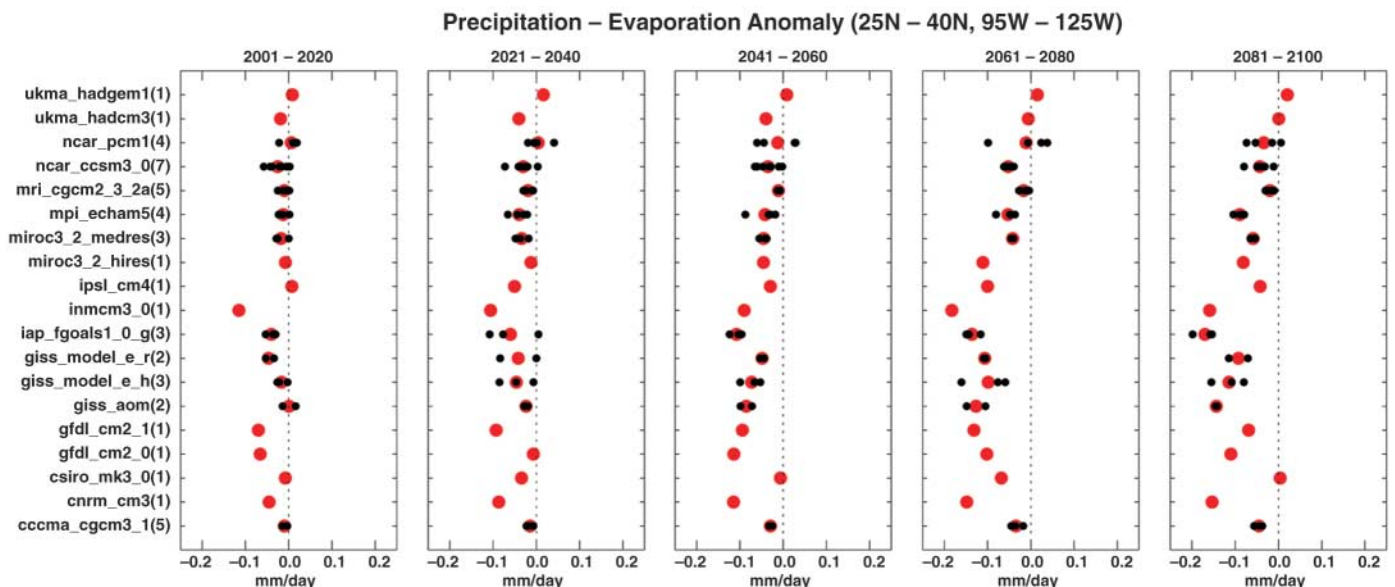


**Fig. 2.** The change in annual mean  $P - E$  over the American Southwest (125°W to 95°W and 25°N to 40°N, land areas only) for 19 models (listed at left), relative to model climatologies from 1950–2000. Results are averaged over 20-year segments

of the current century. The number of ensemble members for each projection is listed by the model name at left. Black dots represent ensemble members (where available), and red dots represent the ensemble mean for each model.

The mean flow convergence term involving only changes in humidity (Fig. 4B) causes increasing  $P - E$  in regions of low-level mean mass convergence and decreasing  $P - E$  in regions of low-level mean mass divergence, generally intensifying the existing pattern of  $P - E$  (6). This term helps to explain much of the reduction in  $P - E$  over the subtropical oceans, where there is strong evaporation, atmospheric moisture divergence, and low precipitation (6). Over land areas in general, there is no infinite surface-water source, and  $P - E$  has to be positive and sustained by atmospheric moisture convergence. Over the American Southwest, in the current climate, it is the time-varying flow that sustains most of the positive  $P - E$ , whereas the mean flow diverges moisture away. Here, the “humidity contribution” leads to reduced  $P - E$ , as the moisture divergence by the mean flow increases with rising humidity. Over the Mediterranean region, there is mean moisture divergence, and rising humidity again leads to increased mean moisture divergence and reduced  $P - E$ .

Over the ocean, the contribution of humidity changes to changes in  $P - E$  can be closely approximated by assuming that the relative humidity remains fixed at its 1950–2000 values (6). Over almost all land areas and especially over those that have reduced  $P - E$ , the relative humidity decreases in the early 21st century. This is be-

cause, unlike over the ocean, evaporation cannot keep pace with the rising saturation humidity of the warming atmosphere. Over land, the humidity contribution to the change in  $P - E$  is distinct from that associated with fixed relative humidity.

Decreases in  $P - E$  can also be sustained by changes in atmospheric circulation that alter the mean moisture convergence, even in the absence of changes in humidity (Fig. 4A). This “mean circulation contribution” leads to reduced  $P - E$  at the northern edge of the subtropics (e.g., the Mediterranean region, the Pacific and the Atlantic around 30°N, and parts of southwestern North America). The change in moisture convergence by the transient eddies (Fig. 4C) dries southern Europe and the subtropical Atlantic and moistens the higher-latitude Atlantic, but it does not have a coherent and large impact over North America.

A substantial portion of the mean circulation contribution, especially in winter, can be accounted for by the change in zonal mean flow alone (not shown in the figures), indicating that changes in the Hadley Cell and the extratropical mean meridional circulation are important. Increases in humidity and mean moisture divergence, changes in atmospheric circulation, and the intensification of eddy moisture divergence cause drying in the subtropics, including the area over western North America and the Med-

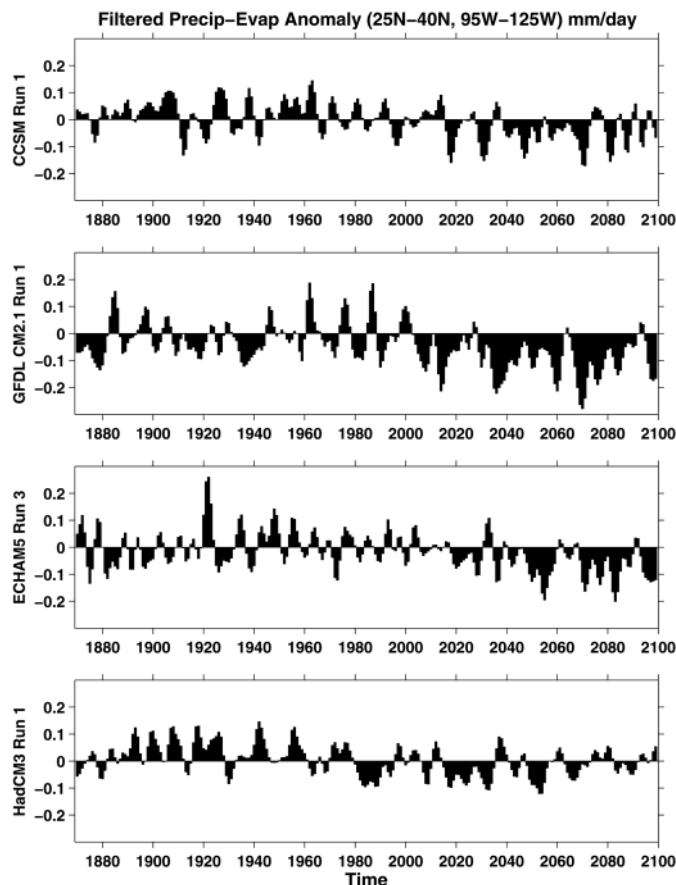
iterranean region. For the Southwest region, the annual mean  $P - E$  decreases by 0.086 mm/day, which is largely accounted for by an increase in the mean flow moisture divergence. Changes in the circulation alone contribute 0.095 mm/day of drying, and changes in the humidity alone contribute 0.032 mm/day. These changes are modestly offset by an increased transient-eddy moisture convergence of 0.019 mm/day. (7).

Within models, the poleward edge of the Hadley Cell and the mid-latitude westerlies move poleward during the 21st century (8–10). The descending branch of the Hadley Cell causes aridity, and hence the subtropical dry zones expand poleward. In models, a poleward circulation shift can be forced by rising tropical sea surface temperatures (SSTs) in the Indo-Pacific region (11) and by uniform surface warming (12). The latter results are relevant because the spatial pattern of surface warming in the AR4 models is quite uniform away from the poles. One explanation (13, 14) is that rising tropospheric static stability, an established consequence of moist thermodynamics, stabilizes the subtropical jet streams at the poleward flank of the Hadley Cell against baroclinic instability. Consequently, the Hadley Cell extends poleward (increasing the vertical wind shear at its edge) to a new latitude where the shear successfully compensates for the suppression of baroclinic instability by rising static stability.

Although increasing stability is likely to be a substantial component of the final explanation, a fully satisfying theory for the poleward shift of the zonal mean atmospheric circulation in a warming world must account for the complex interplay between the mean circulation (Hadley Cell and the mid-latitude Ferrell Cell) and the transient eddies (13, 14) that will determine where precipitation will increase and decrease in the future. However, not all of the subtropical drying in the Southwest and Mediterranean regions can be accounted for by zonally symmetric processes, and a full explanation will require attention to moisture transport within localized storm tracks and stationary waves.

The six severe multiyear droughts that have struck western North America in the instrumental record have all been attributed (by the use of climate models) to variations in SSTs in the tropics, particularly persistent La Niña-like SSTs in the tropical Pacific Ocean (15–19). The projected future climate of intensified aridity in the Southwest is caused by different processes, because the models vary in their tropical SST response to anthropogenic forcing. Instead, it is caused by rising humidity that causes increased moisture divergence and changes in atmospheric circulation cells that include a poleward expansion of the subtropical dry zones. The drying of subtropical land areas that, according to the models, is imminent or already under way is unlike any climate state we have seen in the instrumental record. It is also distinct from the multidecadal megadroughts that afflicted the American Southwest during Medieval times (20–22), which have also been attributed to changes in tropical SSTs (18, 23). The most severe

**Fig. 3.** The change in annual mean  $P - E$  over the American Southwest (125°W to 95°W and 25°N to 40°N, land areas only) for four coupled models, relative to model ensemble mean climatologies from 1950–2000. The results are from individual simulations of the 1860–2000 period, forced by known and estimated climate forcings and individual projections of future climate with the SResA1B scenarios of climate forcings. Because the modeled anomalies have not been averaged together here, these time series provide an idea of plausible evolutions of Southwest climate toward a more arid state. The models are the National Center for Atmospheric Research Community Climate System Model (CCSM), GFDL model CM2.1, Max Planck Institut Für Meteorologie model ECHAM5, and Hadley Centre for Climate Change model HadCM3. All time series are for annual mean data, and a 6-year low-pass Butterworth filter has been applied.



**Contributions to Change in Moisture Convergence  
(2021 – 2040) – (1950 – 2000)**

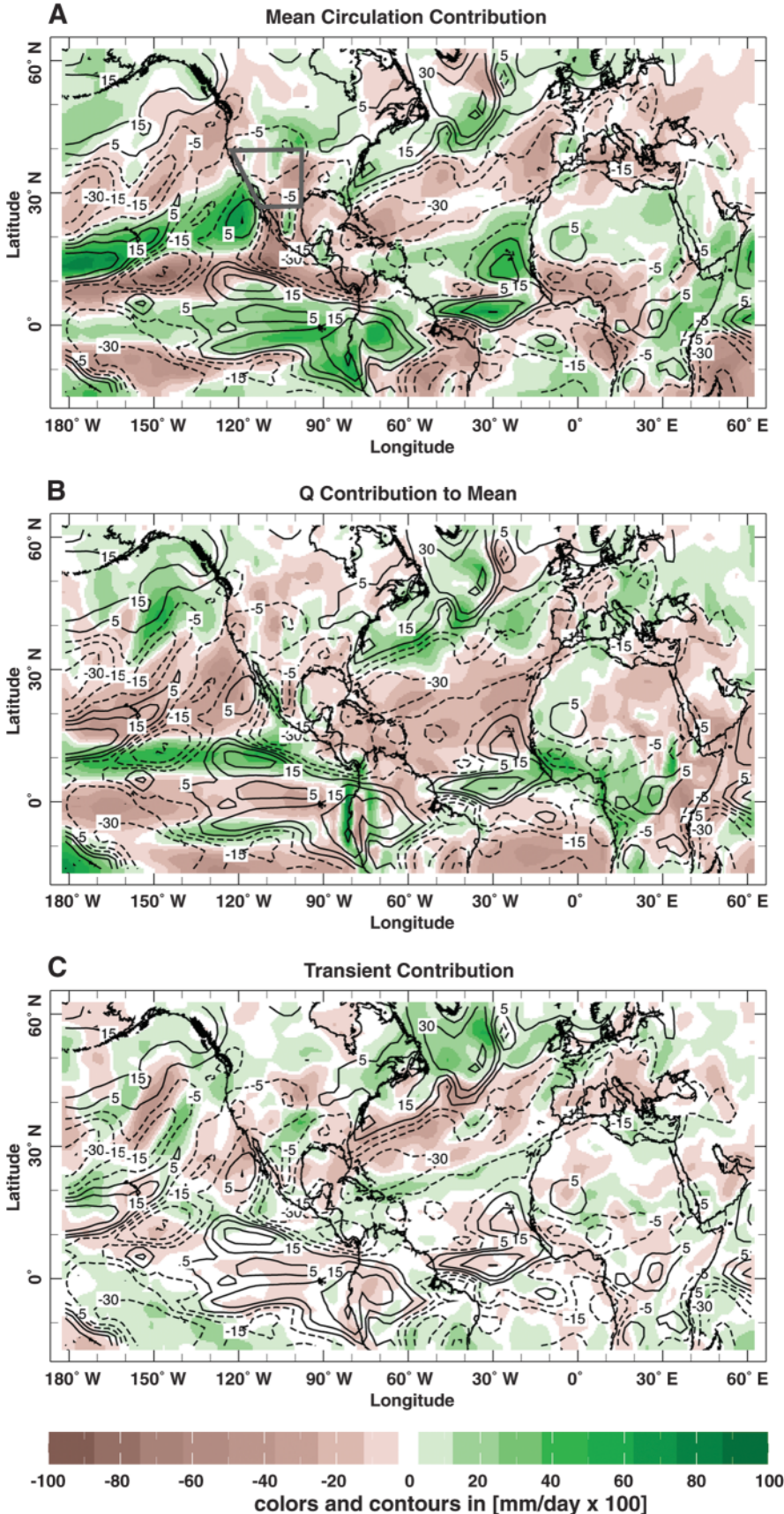


**Fig. 4.** The change in annual means of  $P - E$  for the 2021–2040 period minus the 1950–2000 period [contours in (A) to (C)] and contributions to the change in vertically integrated moisture convergence (colors; negative values imply increased moisture divergence) by the mean flow, due to (A) changes in the flow, (B) the specific humidity, and (C) the transient-eddy moisture convergence, all for the GFDL CM2.1 model. The box in (A) shows the area we defined as “the Southwest.”

future droughts will still occur during persistent La Niña events, but they will be worse than any since the Medieval period, because the La Niña conditions will be perturbing a base state that is drier than any state experienced recently.

**References and Notes**

1. U. Cubasch *et al.*, in *Climate Change 2000—The Scientific Basis: Contribution of Working Group I to the Third Assessment Report of the Intergovernmental Panel on Climate Change*, J. T. Houghton *et al.*, Eds. (Cambridge Univ. Press, Cambridge, 2001), pp. 525–582.
2. M. R. Allen, W. J. Ingram, *Nature* **419**, 224 (2002).
3. Details of the models analyzed can be found at [www-pcmdi.llnl.gov/ipcc/model\\_documentation/ipcc\\_model\\_documentation.php](http://www-pcmdi.llnl.gov/ipcc/model_documentation/ipcc_model_documentation.php), and the data can be found at <https://esg.llnl.gov:8443/index.jsp>.
4. N. Nakicenovic, R. Swart, Eds., *Special Report on Emissions Scenarios* (Cambridge Univ. Press, New York, 2000).
5. T. L. Delworth *et al.*, *J. Clim.* **19**, 643 (2006).
6. I. M. Held, B. J. Soden, *J. Clim.* **19**, 5686 (2006).
7. The model  $P - E$  is not fully accounted for by the computed moisture flow convergence that is calculated by taking the sum of the components of the mean flow and transient eddies (the imbalance is 0.022 mm/day). Calculations were performed with data collected daily on the model grid using closely matching numerics, but errors could be introduced by not using a time resolution of several hours and by neglecting moisture diffusion (potentially large over mountains), which was not archived. The data are available at <http://kage.ldeo.columbia.edu/SOURCES/LDEO/ClimateGroup/GFDL>.
8. J. H. Yin, *Geophys. Res. Lett.* **32**, L18701 (2005).
9. P. J. Kushner, I. M. Held, T. L. Delworth, *J. Clim.* **14**, 2238 (2001).
10. L. Bengtsson, K. I. Hodges, E. Roeckner, *J. Clim.* **19**, 3518 (2006).
11. N.-C. Lau, A. Leetmaa, M. J. Nath, *J. Clim.* **19**, 3607 (2006).
12. S. Lee, *J. Atmos. Sci.* **56**, 1353 (1999).
13. T. Schneider, *Annu. Rev. Earth Planet. Sci.* **34**, 655 (2006).
14. C. C. Walker, T. Schneider, *J. Atmos. Sci.* **63**, 3333 (2006).
15. S. D. Schubert, M. J. Suarez, P. J. Pegion, R. D. Koster, J. T. Bacmeister, *Science* **303**, 1855 (2004).
16. S. D. Schubert, M. J. Suarez, P. J. Pegion, R. D. Koster, J. T. Bacmeister, *J. Clim.* **17**, 485 (2004).
17. R. Seager, Y. Kushnir, C. Herweijer, N. Naik, J. Velez, *J. Clim.* **18**, 4065 (2005).
18. C. Herweijer, R. Seager, E. R. Cook, *Holocene* **16**, 159 (2006).
19. H.-P. Huang, R. Seager, Y. Kushnir, *Clim. Dyn.* **24**, 721 (2005).
20. S. Stine, *Nature* **369**, 546 (1994).
21. E. R. Cook, C. A. Woodhouse, C. M. Eakin, D. M. Meko, D. W. Stahle, *Science* **306**, 1015 (2004).
22. C. Herweijer, R. Seager, E. R. Cook, J. Emile-Geay, *J. Clim.* **20**, 1353 (2007).
23. E. R. Cook, R. Seager, M. A. Cane, D. W. Stahle, *Earth Sci. Rev.* **81**, 93 (2007).
24. This work was supported at LDEO by NOAA grants NA03OAR4320179 and NA06OAR4310151 and by NSF grants ATM05-01878, ATM04-34221, and ATM03-47009. We thank R. Dole, W. Robinson, and M. Wallace for useful conversations.

5 January 2007; accepted 26 March 2007

Published online 5 April 2007;

10.1126/science.1139601

Include this information when citing this paper.